Determination of activation parameters for the core transformation of the screw dislocation in silicon

2010 Modelling Simul. Mater. Sci. Eng. 18 065001

(http://iopscience.iop.org/0965-0393/18/6/065001)

Modelling Simul. Mater. Sci. Eng. **18** (2010) 065001 (11pp) doi:10.1088/0965-0393/18/6/065001

Determination of activation parameters for the core transformation of the screw dislocation in silicon

J Guénolé, J Godet and L Pizzagalli

Institut Pprime, CNRS - Université de Poitiers - ENSMA, SP2MI, B.P. 30179, 86962 Futuroscope Chasseneuil Cedex, France

E-mail: Laurent.Pizzagalli@univ-poitiers.fr

Received 9 February 2010, in final form 11 May 2010
Published 24 June 2010
Online at stacks.iop.org/MSMSE/18/065001

Abstract

The non-dissociated screw dislocation in a model covalent material like silicon is known to exist in three possible stable core configurations. We performed calculations combining the nudged elastic band technique and a semi-empirical description in order to determine mechanisms and activation parameters for transforming one core into another. Our results showed that a glide core is necessarily reconstructed, since the energy barrier for reconstruction is easily overcome by thermal activation. Conversely, a transformation between a shuffle and a glide core appears unlikely at low temperature, which raises questions about the existence of the double-period glide configuration.

(Some figures in this article are in colour only in the electronic version)

1. Introduction

It is well known that the plasticity properties of covalent materials are considerably dependent on the structure of the dislocation cores. Owing to the strong directionality of bonds in these materials, dislocation cores often exhibit reconstruction. In silicon for instance, which is usually considered as a model covalent material, the cores of 30° and 90° partial dislocations are both reconstructed [1–3]. For similar reasons, several stable core configurations are also possible for a given kind of dislocation. Hence, the 90° partial dislocation was shown to occur in two possible configurations, almost degenerate in energy in silicon [4–7]. This issue is also common to perfect dislocation cores in silicon [8]. For the 60° dislocation core, two stable and one metastable configurations were recently proposed [9]. For the screw dislocation, in addition to earlier core suggestions by Hornstra [10], a third configuration was obtained on the basis of first-principles calculations [11]. The multiplicity of possible core structures is a real issue, since one has to assess which one is important for determining the mobility of the dislocation.

To circumvent this problem, one may first find out which one of the dislocation cores is the most stable, then investigates the mobility properties of the winner. It is not certain

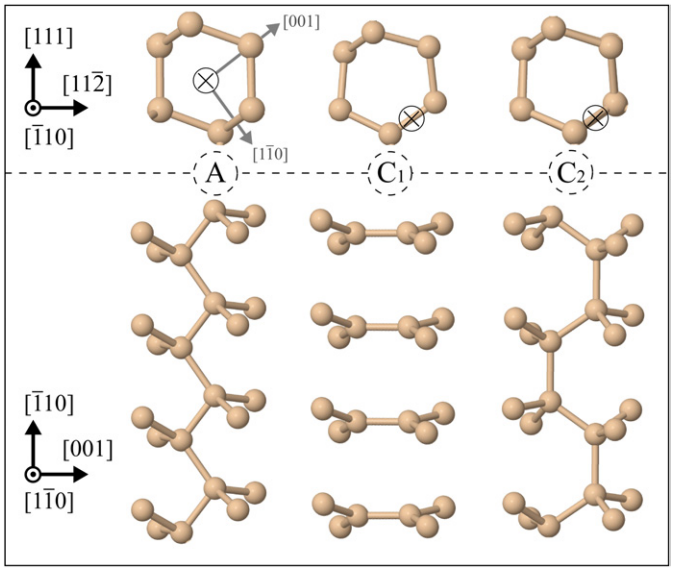

Figure 1. Ball-stick representation of the three screw dislocation configurations used in the calculations. Top: projection along [$\bar{1}$ 1 0], the dislocation line; the screw dislocation line location is marked by a circled cross. Bottom: projection along [1 $\bar{1}$ 0].

that such a procedure is always appropriate for dislocations. In fact, the most stable core configuration can be largely reconstructed and associated with very deep Peierls valleys, and be hard to displace as a consequence. Other core configurations, with higher energy but more mobile, could therefore be important as well. In other words, the important question regarding dislocation core in covalent materials is whether the more stable or the more mobile one will govern the mobility of a given dislocation. The case of the screw dislocation in silicon allows for a good illustration of the issue. In fact, in the current state of knowledge, three stable or metastable core configurations were determined[1]. One[2] (C_1) corresponds to a dislocation centered at the intersection of two {1 1 1} planes[3] in the glide set (figure 1), and was shown to be weakly stable [8]. It can reconstruct into a very stable core configuration, C_2, which exhibits a double period along the dislocation line [11]. Finally, a third stable configuration, A, is obtained when the dislocation is centered at the intersection of two {1 1 1} planes in the shuffle set (figure 1). A is more stable than C_1 but less than C_2 [11, 12]. Regarding mobility, first-principles calculations showed that the Peierls stress for the A core is 4 GPa [13], whereas it is 6 GPa for the C_2 core [11]. The displacement of the A core by kinks pairs mechanism was also recently investigated [14], suggesting that thermally activated motion of the A core is very likely in conditions where dislocations are non-dissociated in silicon [8]. It seems that the most stable C_2 core is less mobile than the A core, and it is not clear which core is the most important one for the plasticity properties of silicon.

To determine the respective role of each core, information about the possible transformation from one configuration to the other would be highly valuable. For instance, the transformation A $\Leftrightarrow$ C_2 is a key mechanism if one considers that the screw dislocation is

[1] Note that another high-symmetry configuration has been proposed by Koizumi *et al* [30], but it has been shown that the stability of this geometry was spuriously enhanced by the use of the Stillinger–Weber potential [12].

[2] To label the core configuration in our works, we consider the notation in use in most previous papers.

[3] In the cubic diamond structure, there are two inequivalent {1 1 1} planes, called 'glide' and 'shuffle', respectively, for historical reasons [26].

Table 1. Energy differences (in eV per Burgers vector) between three possible screw dislocation cores in silicon, computed with Tersoff potential and EDIP, tight-binding (TB) and density functional theory (DFT) methods.

	Tersoff	EDIP	TB [11]	DFT [11]	TB [21]	DFT [12]
C_2 | A	0.31	0.07	0.62	0.54	0.60	
C_2 | C_1	0.85	0.81				
A | C_1	0.54	0.74				0.86

in a C_2 configuration at rest, but in a A configuration during motion. Such a transformation would be a kind of unlocking–locking process [15]. Another possible core transformation is $C_1 \Leftrightarrow C_2$, which corresponds to the reconstruction of the screw dislocation along its line. The characterization of these transformations requires the identification of the mechanism and the determination of the associated energy barrier. In addition, in the case of A $\Leftrightarrow C_2$ the dislocation has to slip, and a possible influence of an applied stress on the transformation is expected.

To the best of our knowledge, there is no available information regarding core transformations for non-dissociated dislocations in materials with cubic diamond lattice. To improve the current state of knowledge, we have determined the activation parameters for several possible core transformations, focusing on the perfect screw dislocation in silicon. The transformation mechanisms and its associated energy barrier were computed with a combination of semi-empirical potential and nudged elastic band (NEB) calculations. After describing the model and the methods, we discuss the transformations A $\Leftrightarrow C_1$, $C_1 \Leftrightarrow C_2$ and A $\Leftrightarrow C_2$.

2. Method

Dislocation core transformations were investigated combining the NEB technique [16] and a semi-empirical potential description of silicon cohesion. The choice of this approximate method is dictated by the sizes of the investigated systems, which prevent the use of accurate first-principles calculations. In this work, we considered two different potentials, the Tersoff potential [17] and EDIP [18]. They have been widely used for describing defects in silicon, with a good accuracy [19, 20]. Although one has to be cautious about the use of empirical potentials for modeling dislocations in silicon, we found that these two potentials provide the right ordering for the stability of the different possible core geometries, with C_2 the most stable configuration, followed by A and C_1, respectively. The energy differences between the three dislocation cores are reported in table 1, together with reference data obtained from electronic structure calculations. The Tersoff potential yields the closest energy differences compared with reference data, with an error of at most 0.3 eV. EDIP performance is less satisfactory, with an underestimated energy difference between C_2 and A. In the following, we focus essentially on the Tersoff potential calculations. The optimized lattice parameters for the Tersoff potential and EDIP are 5.432 Å and 5.430 Å, respectively.

In this work, we considered an orthorhombic computational cell, the crystal being orientated along the directions [1 1 1], [1 1 $\bar{2}$] and [$\bar{1}$ 1 0], the latter being the direction of the dislocation line and of the Burgers vector b. The dimensions of the cell are $20 \times 42 \times 10$, i.e. a dimension of $10b$ along [$\bar{1}$ 1 0], and a total number of 8400 silicon atoms. We found that this cell size is small enough to allow efficient and fast NEB calculations, while making dislocation-boundary interactions negligible. Along [$\bar{1}$ 1 0], the dislocation line axis (see figure 1), periodic boundary conditions are applied in order to model an infinite screw dislocation. For the two other directions instead, we used free surfaces. This is an usual modeling framework for dislocation investigations [22]. The different screw dislocation

configurations were obtained by first displacing the atoms of a perfect crystal lattice according to anisotropic elasticity theory, centered on two different locations (figure 1). Then, the residual forces on the system were relaxed using a conjugated gradient algorithm until convergence. The C_2 configuration is obtained from C_1, with a manual rearrangement of dislocation core atoms prior to relaxation.

Three different core transformations, A $\Leftrightarrow$ C_1, C_1 $\Leftrightarrow$ C_2 and A $\Leftrightarrow$ C_2, were investigated using NEB calculations. The transformation from one core to another was made gradually, in a process similar to the formation of a pair of kinks and the migration of one of the kinks [14]. For instance, starting from configuration A, the system encompasses 10 identical [$\bar{1}$ 1 0] layers of width b with a core A. We built a first intermediate configuration by replacing one A core layer with a C_1 core layer. The configuration is then relaxed and used as a stable point in the NEB calculations. Successive intermediate configurations were built in the same way by increasing the number of C_1 core layers. When all 10 layers have been replaced, an infinite C_1 screw dislocation is obtained. In the case of the C_2 core configuration, which exhibits a two [$\bar{1}$ 1 0] layers period, intermediate configurations are obviously generated by replacing cores in two layers. It has to be noted that all these intermediate configurations were found to be stable, for all investigated core transformations. NEB calculations were performed with eight optimized images between each intermediate configurations for the A $\Leftrightarrow$ C_1 and C_1 $\Leftrightarrow$ C_2 transformation and 28 in the case of the A $\Leftrightarrow$ C_2 transformation. We used the improved tangent algorithm [23] and the climbing image technique [24] in order to improve the accuracy of the saddle point determination during NEB calculations. At last, NEB calculations were considered converged when every residual forces were below 10^{-2} eV Å^{-1}.

The effect of stress on core transformations was investigated by applying a shear strain on the system. [1 1 1] surfaces were frozen and rigidly shifted in order to set and sustain the strain. We used a shear strain for which the stress relaxation is maximum during the A $\Leftrightarrow$ C_2 core transformation. This is obtained by shearing (0 0 1) planes encompassing both A and C_2 dislocation cores along the Burgers vector orientation [$\bar{1}$ 1 0] (figure 1). Our investigations were made for strain magnitudes of at most 5%, and with the Tersoff potential.

3. A $\Leftrightarrow$ C_1

First, we investigated the dislocation core displacement from configurations A to C_1. A prior analysis of both dislocation geometries is helpful to understand the core transformation. Projected on a ($\bar{1}$ 1 0) plane, the cubic diamond lattice is characterized by hexagons (figure 1), which seemingly include 4 'long' bonds and 2 'short' bonds. Obviously, this is a simple effect of projection, atoms forming 'long' bonds being in the same ($\bar{1}$ 1 0) plane whereas those forming 'short' bonds are separated by $a_0/2\sqrt{2}$ (one half of the Burgers vector) along the $\langle\bar{1}\,1\,0\rangle$ direction. The two atoms forming 'short' bonds will experience the maximum displacements in all the investigated dislocation core transformations. Therefore, they can be used to characterize the geometrical changes. In the following, they will be called 'core' atoms.

In the case of the dislocation configuration A, the core atoms are bound like in bulk, the maximum deformation being located in the center of the hexagon (figure 1). Conversely, in the case of the configuration C_1, the center of the strain field is located between two core atoms. This leads to the alternative up and down displacements along $\langle\bar{1}\,1\,0\rangle$ of these atoms, resulting in a bond contained in the ($\bar{1}$ 1 0) plane (figure 1). After this reorganization, core atoms are 3-fold coordinated, with almost coplanar bonds. This geometry is representative of a local sp^2 electronic structure, instead of the usual sp^3 hybridization of silicon. The transformation from configurations A to C_1 necessarily involves the breaking of bonds between core atoms.

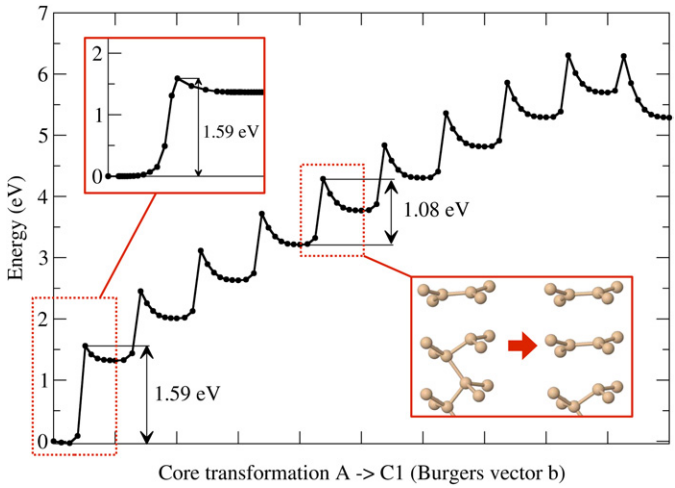

Figure 2. Energy variation associated with the gradual transformation of a screw dislocation core from the A configuration to the C_1 configuration, calculated with the NEB technique and the Tersoff potential. The left insert is a more accurate NEB calculation of the first energy barrier with 38 images. The range of the x-coordinate axis corresponds to the size of the computational cell along the dislocation line direction, the left (right) edge corresponding to a full A (C_1) core, respectively. Energy barriers for initial and intermediate transformation steps are reported in the graph. For the intermediate step, the inset graph shows the initial and final structures along the dislocation line.

Figure 2 shows the energy variation for the gradual transformation of the A core into the C_1 core, the dislocation length being $10b$, calculated with multiple NEB calculations and the Tersoff potential. The general aspect of the curve clearly indicates that the transformation is achieved through successive and equivalent steps. Each elementary step corresponds to the A $\Leftrightarrow$ C_1 transformation of one $[\bar{1}\,1\,0]$ layer (width b). Figure 2 also shows the associated atomistic mechanism when half of the screw dislocation is already in the C_1 configuration. In that case, side effects due to periodic boundary conditions are minimal, and this process is equivalent to a single transformation step along an infinite screw dislocation. The elementary transformation mechanism involves the gradual stretching of a bond between two core atoms, until complete separation. Initially, the bond length between the two core atoms is 2.52 Å. The bond breaking is the saddle point of the transformation in the configuration space, and corresponds to the maximum in the energy variation. This saddle point is characterized by a maximum bond length of 2.96 Å, and an energy barrier of 1.08 eV relative to the initial configuration. Finally the energy decreases to a final energy value of 0.56 eV above the initial state, following the relaxation of the new geometry. This value is very close to the energy difference between A and C_1 core configurations (table 1). The important value here is obviously the energy barrier. To check the influence of the potential on this quantity, we performed calculations with EDIP and found an energy barrier of 1.01 eV, therefore in very good agreement.

A significantly larger energy barrier of 1.59 eV is required to initiate the transformation starting from a full A core. This first elementary step is alike the formation of the narrowest possible kinks pair bridging Peierls valleys for A and C_1 screw dislocations, with separation b. Nevertheless, the atomistic mechanism is very similar to one of the next steps, the saddle point corresponding to a maximum bond length of 2.99 Å. The controlling process for a possible A $\Leftrightarrow$ C_1 core transformation is therefore the first step, since this is the highest energy barrier. Additional calculations with EDIP suggest a slightly lower energy barrier of 1.32 eV.

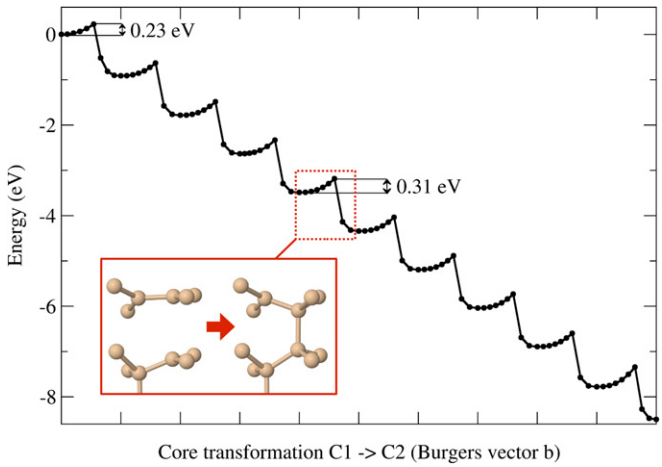

Figure 3. Energy variation associated with the gradual transformation of a screw dislocation core from the C_1 configuration to the C_2 configuration, calculated with the NEB technique and the Tersoff potential. Additional information is included in the caption of figure 2.

In the right side of figure 2, one can see the energy variation for the final elementary step which allows us to recover the full C_1 core. The energy variation pattern appears to be slightly different in that case, as the final configuration has a lower energy than the initial one. This is caused by the use of periodic boundary conditions along the dislocation line.

Overall, the transition mechanisms are characterized by sharp energy increases, although they correspond to small atomic displacements. We have checked that these energy jumps were not due to an insufficient number of images in our NEB calculations. Performing additional calculations with 38 images (figure 2), we obtained an equivalent energy curve with precisely the same energy barrier, as expected. A likely explanation for these sharp energy variations is the use of semi-empirical potentials for describing Si–Si bond breakings, a feature already mentionned in gamma surfaces calculations [25].

4. $C_1 \Leftrightarrow C_2$

The recent discovery of the C_2 screw dislocation core by Wang *et al* brought a new interest for glide set dislocation [11]. Although it is clear that the C_2 core has a much lower energy than the C_1 core, the energy barrier for the double-period reconstruction along the dislocation line is not known. We have performed calculations in a similar way than previously for investigating this transformation. In that case, there is no displacement of the dislocation line, and an applied stress is expected to have no influence on the outcome.

Figure 3 represents the energy variation for the gradual transformation from the C_1 core into the C_2 core, following the same methodology than in the previous section. Again, it is clear that the complete transformation is obtained after several successive equivalent steps, each one allowing for the conversion of a dislocation segment of width b. One of these steps, minimizing side effects due to periodic conditions, is shown in figure 3. In the initial configuration, core atoms along the dislocation line direction $[\bar{1}\,1\,0]$ (see figures 1 and 3) are separated by 3.89 Å, very close to b. Then two of these atoms, on top of each other along $[\bar{1}\,1\,0]$ are progressively brought together, until the formation of a bond. This process is not the reverse of the elementary mechanism of the $A \Leftrightarrow C_1$ transformation, since bonded core atoms are not on top of each other along $[\bar{1}\,1\,0]$ in the A configuration (figure 1). Here, the atoms are initially closer, thus reducing

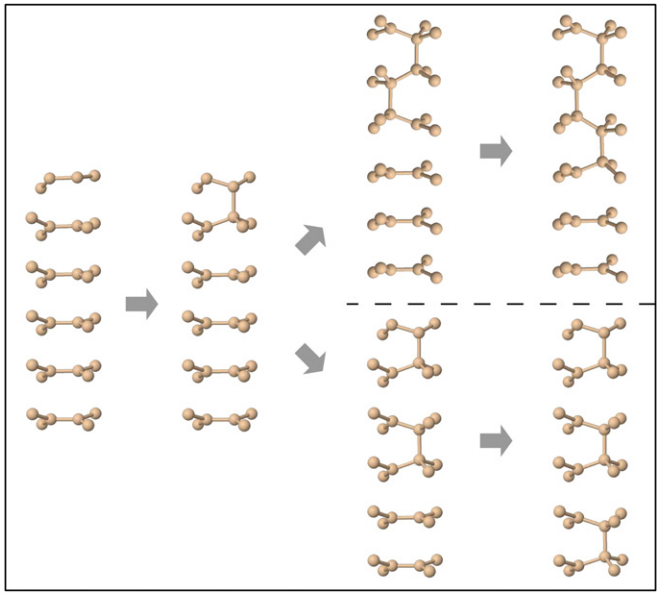

Figure 4. Two possible paths for reconstructing a C_1 screw dislocation core into C_2: the staggered row process (upper part) and the asymmetric partial process (lower part).

the strain required to make the bond between core atoms. As a consequence, the energy barrier is also low, with a value of 0.31 eV. It corresponds to a saddle configuration in which the two core atoms are separated by 2.96 Å. In the final configuration, the bond length between the two core atoms is 2.45 Å, i.e. almost equal to the first neighbor distance in bulk silicon. The energy gained during an intermediate transformation step is 0.85 eV. As anticipated, this value is equal to the energy difference between C_1 and C_2 configurations for an infinite screw dislocation. Calculations performed with EDIP are in agreement with a computed energy barrier of 0.17 eV.

Conversely to the A $\Leftrightarrow$ C_1 transformation, the initial step requires to overcome an energy barrier which is lower than the following steps. In fact, the calculated saddle point corresponds to an energy value of 0.23 eV. With EDIP, we obtained a very low energy of 0.08 eV. The controlling process is therefore not the initiation mechanism, but rather the continuation of an already on-going transformation. In any cases, the energies involved in the transformation are low enough to indicate that the reconstruction from C_1 to C_2 will necessarily happen in usual conditions, e.g. at room temperature. The following conclusion is that a C_1 screw dislocation is very unlikely to exist in silicon.

Up to now, in our $C_1 \Leftrightarrow C_2$ investigations, we have assumed that the successive formation of bonds between core atoms was alternate with respect to the dislocation center (see figure 1). This staggered row process is sketched in the upper part of figure 4. We have also studied a different mechanism, in which only one part of the dislocation core was reconstructed (figure 4, lower part). The minimum energy paths were found to be similar than previously, albeit with lower energy barriers equal to 0.22 eV. The asymmetric partial reconstruction is then slightly favored over the staggered row process. However, since the involved energies are very close, it is likely that the way the dislocation reconstructs has little influence on other properties. The complementary transformation for recovering the complete C_2 configuration was found to be associated with an energy barrier of 0.40 eV.

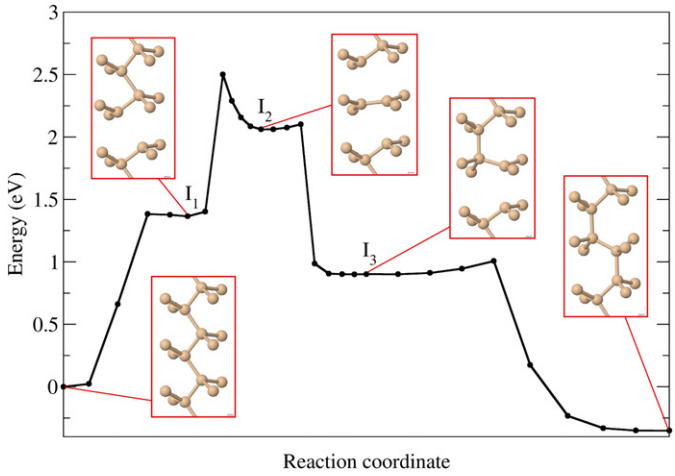

Figure 5. Minimum energy path for the initial step of the A $\Leftrightarrow$ C_2 transformation. The insets represent the initial (A core), the final (A core including a 2*b* segment of C_2 core) and three intermediate metastable configurations.

5. A $\Leftrightarrow$ C_2

The last core transformation, A $\Leftrightarrow$ C_2, is surely the most interesting one regarding the 'glide-shuffle' issue in covalent semiconductors. In fact, while it is well acknowledged that at high temperatures dislocations in silicon are dissociated and are located in 'glide' planes [26], several experiments showed that at low temperature, they are not dissociated [8]. Most of these investigations lead to the conclusion that these non-dissociated dislocations belong to 'shuffle' planes. The necessary transition between high and low temperatures remains largely unknown. Accordingly, the characterization of the transformation between the 'shuffle' core A and the 'glide' core C_2 is expected to bring new insights about such a transition.

Compared with previously investigated core transformations, A $\Leftrightarrow$ C_2 is more complex since it combines displacement and reconstruction of the core. Due to the double periodicity of the C_2 configuration, a single transformation step will concern a dislocation segment of length 2*b*. The optimized minimum energy path calculated using the Tersoff potential for the first transformation step is shown in figure 5. Starting from the initial configuration including a full A core, the breaking of one bond is achieved through the gradual separation of two core atoms, leading to the first intermediate configuration I_1. This mechanism is associated with an energy barrier of 1.38 eV, and is similar to the elementary process for the A $\Leftrightarrow$ C_1 core transformation. Then, a second bond, linking two other core atoms (located at a distance *b* compared with the previous ones), is broken. The associated energy barrier to overcome is 1.13 eV. The second intermediate configuration I_2 appears to be composed of one C_1 dislocation segment of width *b*, enclosed in a A core. The third intermediate configuration I_3 is easily obtained, with a very small energy barrier of 0.04 eV. The atomistic mechanism is alike the elementary process of the C_1 $\Leftrightarrow$ C_2 core transformation, with the formation of a bond between two core atoms on top of each other (figure 5). A similar transition allowing the formation of a second bond with a low energy barrier of 0.10 eV, finally leads to the final configuration. At the end we have now a C_2 dislocation segment of width 2*b* enclosed in a A core. The total energy barrier, i.e. the highest point along the minimum energy path in figure 5, is 2.50 eV. Using EDIP, a similar mechanism is obtained, with a computed total energy barrier of 2.31 eV in very good agreement.

The transformation of a dislocation segment of width $2b$ between A and C_2 configurations is obtained thanks to four mechanisms which occur in succession. The first two are similar to the elementary step of the A $\Leftrightarrow$ C_1 core transformation, while the last two are equivalent to bond formation events as obtained in the C_1 $\Leftrightarrow$ C_2 transformation. The A $\Leftrightarrow$ C_1 mechanism is activated with a high energy barrier, ranging from 1.08 to 1.59 eV. The high energy barrier of the A $\Leftrightarrow$ C_2 transformation is then coherent since A $\Leftrightarrow$ C_2 first requires the activation of two A $\Leftrightarrow$ C_1 mechanisms in succession. One may wonder whether it could be possible to change the sequence of the four mechanisms with an alternance of A $\Leftrightarrow$ C_1 and C_1 $\Leftrightarrow$ C_2 processes, in order to obtain a lower activation energy. However, a simple geometry analysis shows that such an atomic rearrangement is highly unlikely, since it would require an intermediate configuration with two 5-fold coordinated core atoms and another 3-fold coordinated one. Accordingly, the best mechanism, i.e. with the lowest activation energy, is the one we found. It includes the rotation of a core atoms dimer along the $[1\,\bar{1}\,0]$ axis, which can be obtained solely through the successive breaking of two bonds.

What is described above is the first step of the A $\Leftrightarrow$ C_2 transformation. Our investigations showed that the full transformation is achieved by repeating this step. The total energy barrier is significantly reduced to 1.90 eV for the next steps compared with the initial one. This is a consequence of a lowering of the first energy barrier and an improved stability of the intermediate configuration I_1. A similar feature is observed in results obtained with EDIP, with a reduction in the total energy barrier from 2.31 eV for the first step to 1.89 eV for the following ones.

The limiting step for the complete transformation between A and C_2 cores is therefore the initial one. On the basis of our calculations with two different potentials, the energy barrier is ranging from 2.3 to 2.5 eV. An estimation of the time for a successful transition to occur can be obtained in the framework of transition state theory [27]. Here we target a timescale of 1 s for the initial step process. In fact, the initial step is the limiting one and controls the kinetics of the complete core transformation. This situation is different from the displacement of dislocations through formation and migration of kinks, for which a large number of events are required for displacing the dislocation during deformation experiments. Using a standard attempt frequency of 10^{13} s^{-1}, we determined that one successful event will be obtained for temperatures between 900 and 970 K. Comparing these values with the temperature range characterizing the transition between non-dissociated and partial dislocations regimes in silicon, it is found that they are slightly larger than in the experiments [8], and in the same range obtained by molecular dynamics simulations of dislocation nucleation with the same potentials [28]. Therefore, our investigations support the idea that a stable C_2 dislocation configuration could not be obtained from the A core. Indeed, the temperatures needed to activate the transformation are close or larger than temperatures for which non-dissociated dislocations are not present anymore. Nevertheless, the possibility of a nucleation at low temperature of C_2 dislocations cannot be excluded, thanks to an unknown mechanism that could include a C_1 $\Leftrightarrow$ C_2 reconstruction. Previous calculations exclude surface nucleation as a possible option though [29]. Also, regarding the dissociation of screw dislocations at high temperature, one can imagine that the A $\Leftrightarrow$ C_2 transformation is part of the full process.

The effect of stress on the initial step of the A $\Leftrightarrow$ C_2 transformation was also studied, in the case of the Tersoff potential. We found that the activation energy decreases upon the action of the stress, but that the magnitude of the effect is rather small. In fact, an energy barrier reduction of 0.05 eV per per cent of shear strain[4] was determined, for strains up to 5%. Therefore it

[4] Each per cent of strain corresponds to a stress increment of 0.45 GPa when using the Tersoff potential.

appears that the presence or not of stress will not significantly change our previous conclusions regarding the existence of C_2 configuration obtained from the transformation A $\Leftrightarrow$ C_2.

6. Conclusion

We identified the transformation mechanisms between the possible screw dislocation configurations in silicon and determined the associated activation parameters by performing NEB calculations in a semi-empirical framework. The most salient results concern the transformations $C_1 \Leftrightarrow C_2$ and A $\Leftrightarrow$ C_2. First, we showed that a C_1 core will be transformed in C_2 by thermal activation in usual conditions such as room temperature, since the energy barrier for the $C_1 \Leftrightarrow C_2$ transformation is close or lower than 0.3 eV. A C_1 configuration is then rather unlikely in silicon. Second, the A $\Leftrightarrow$ C_2 transformation requires a high energy barrier, ranging from 2.3 to 2.5 eV. An appropriate applied stress contributes to reduce this energy, but the effect is pretty small. Overall, the formation of the C_2 core from the A core appears rather improbable, since required temperatures are above the temperature range for which non-dissociated dislocations were observed. It is possible that the A $\Leftrightarrow$ C_2 is part of a larger process allowing the transformation from the A core to partial dislocations, the C_2 core being an intermediate configuration during dissociation. Finally our results also confirmed that a glide-shuffle transformation in the high stress/low temperature domain is doubtful.

Acknowledgments

This work was supported by the SIMDIM project under contract No ANR-06-BLAN-250. Sandrine Brochard is gratefully acknowledged for encouragement during the redaction of this paper.

References

[1] Duesbery M S, Joos B and Michel D J 1991 Dislocation core studies in empirical silicon models *Phys. Rev.* B **43** 5143
[2] Bulatov V V, Yip S and Argon A S 1995 Atomic modes of dislocation mobility in silicon *Phil. Mag.* A **72** 453
[3] Cai W, Bulatov V V, Chang J, Li J and Yip S 2004 Dislocation core effects on mobility *Dislocations in Solids* vol 12 ed F R N Nabarro and J P Hirth (Amsterdam: North-Holland) p 1 chapter 64
[4] Bennetto J, Nunes R W and Vanderbilt D 1997 Period-doubled structure for the 90° partial dislocation in silicon *Phys. Rev. Lett.* **79** 245
[5] Lehto N and Öberg S 1998 Effects of dislocation interactions: application to the period-doubled core of the 90° partial in silicon *Phys. Rev. Lett.* **80** 5568
[6] Valladares A, White J A and Sutton A P 1998 First principles simulations of the structure, formation, and migration energies of kinks on the 90° partial dislocation in silicon *Phys. Rev. Lett.* **81** 4903
[7] Miranda C R, Nunes R W and Antonelli A 2003 Temperature effects on dislocation core energies in silicon and germanium *Phys. Rev.* B **67** 235201
[8] Rabier J, Pizzagalli L and Demenet J-L 2010 Dislocations in silicon at high stress *Dislocation in Solids* vol 16 ed L Kubin and J P Hirth (Amsterdam: Elsevier) p 47 chapter 93
[9] Pizzagalli L, Godet J and Brochard S 2009 Glissile dislocations with transient cores in silicon *Phys. Rev. Lett.* **103** 065505
[10] Hornstra J 1958 Dislocations in the diamond lattice *J. Phys. Chem. Solids* **5** 129
[11] Wang C-Z, Li J, Ho K-M and Yip S 2006 Undissociated screw dislocation in si: Glide or shuffle set? *Appl. Phys. Lett.* **89** 051910
[12] Pizzagalli L, Beauchamp P and Rabier J 2003 Undissociated screw dislocations in silicon: calculations of core structure and energy *Phil. Mag.* A **83** 1191
[13] Pizzagalli L and Beauchamp P 2004 First principles determination of the peierls stress of the shuffle screw dislocation in silicon *Phil. Mag. Lett.* **84** 729

[14] Pizzagalli L, Pedersen A, Arnaldsson A, Jónsson H and Beauchamp P 2008 Theoretical study of kinks on screw dislocation in silicon *Phys. Rev.* B **77** 064106
[15] Caillard D and Martin J L 2003 *Thermally Activated Mechanisms in Crystal Plasticity (Pergamon Materials Series)* (Oxford: Pergamon)
[16] Jónsson H, Mills G and Jacobsen K W 1998 Nudged elastic band method for finding minimum energy paths of transitions *Classical and Quantum Dynamics in Condensed Phase Simulations* ed B J Berne *et al* (Singapore: World Scientific) p 385 chapter 16
[17] Tersoff J 1989 Modeling solid-state chemistry: interatomic potentials for multicomponent systems *Phys. Rev.* B **39** 5566
[18] Bazant M Z, Kaxiras E and Justo J F 1997 Environment-dependent interatomic potential for bulk silicon *Phys. Rev.* B **56** 8542
[19] Balamane H, Halicioglu T and Tiller W A 1992 Comparative study of silicon empirical interatomic potentials *Phys. Rev.* B **46** 2250
[20] Justo J F, Bazant M Z, Kaxiras E, Bulatov V V and Yip S 1998 Interatomic potential for silicon defects and disordered phases *Phys. Rev.* B **58** 2539
[21] Pizzagalli L, Demenet J L and Rabier J 2009 Theoretical study of pressure effect on the dislocation core properties in semiconductors *Phys. Rev.* B **79** 045203
[22] Bulatov V V and Cai W 2006 *Computer Simulations of Dislocations (Oxford Series on Materials Modelling)* (New York: Oxford University Press)
[23] Henkelman G and Jónsson H 2000 Improved tangent estimate in the nudged elastic band method for finding minimum energy paths and saddle points *J. Chem. Phys.* **113** 9978
[24] Henkelman G, Uberuaga B P and Jónsson H 2000 A climbing image nudged elastic band method for finding saddle points and minimum energy paths *J. Chem. Phys.* **113** 9901
[25] Godet J, Pizzagalli L, Brochard S and Beauchamp B 2003 Comparison between classical potentials and ab initio methods for silicon under large shear *J. Phys.: Condens. Matter* **15** 6943
[26] Hirth J P and Lothe J 1982 *Theory of Dislocations* (New York: Wiley)
[27] Vineyard G H 1957 Frequency factors and isotope effects in solid state rate processes *J. Phys. Chem. Solids* **3** 121
[28] Godet J, Hirel P, Brochard S and Pizzagalli L 2009 Dislocation nucleation from surface step in silicon: the glide set versus the shuffle set *Phys. Status Solidi* a **206** 1885
[29] Godet J, Hirel P, Brochard S and Pizzagalli L 2009 Evidence of two plastic regimes controlled by dislocation nucleation in silicon nanostructures *J. Appl. Phys.* **105** 026104
[30] Koizumi H, Kamimura Y and Suzuki T 2000 Core structure of a screw dislocation in a diamond-like structure *Phil. Mag.* A **80** 609